Application of an Elasto- Plastic Model to Soils Reinforced by Geosynthetics

김은라[1], Eun-ra Kim, Atsushi Iizuka[2], Katsuyuki Kawai[3], 김유성[4], You-song Kim

[1] 일본 Kobe 대학 토목공학과 박사과정, Graduate student. Graduate School of Science and Technology, Kobe University

[2] 일본 Kobe 대학 토목공학과 조교수, Associate Professor, Department of Architecture and Civil Engineering, Kobe University

[3] 일본 Kobe 대학 토목공학과 조수, Instructor, Department of Architecture and Civil Engineering, Kobe University

[4] 전북대학교 토목공학과 부교수, Associate Professor, Department of Civil Engineering, Chonbuk University

SYNOPSIS : 이 논문는 지오신텍스 보강토 구조물의 보강 메카니즘을 수치계산을 통해 규명하고자 하는 목적으로 쓰여졌다. 이 연구에서는 보강 메카니즘은 전단에 의한 다짐토의 체적 팽창(부의 다일렌탄시)을 지오신텍티스에 의해 구속 억제하는 과정에서 생성되는 효과로 간주하고 있다. 보강 메카니즘의 규명을 위해 1992년 일본 Kanazawa에서 실시된 실모형 실험과 실내 실험 결과를 이용하였으며. 수치계산에서는 다짐토의 다일렌탄시 특성을 표현 가능한 탄소성 구성모델을 이용하여 유한요소(FEM)을 이용하고 있다. 수치 계산에 의해 실모형, 실험 실내실험 결과를 비교 분석 하였다.

Key words : *Geosynthetics, compacted soil, subloading surface, dilatancy, finite element simulation*

1. Introduction

The geosynthetic-reinforced soil structures consist of two elements: one is compacted soil and the other is geosynthetics. The reinforcing effect should not be interpreted as that the strength and rigidity of soil itself are merely supplemented by geosynthetic-reinforcement but be understood as that soils and the geosynthetics are unified and show their fresh strength and rigidity as a composite material. The strength and rigidity of geosynthetic-reinforced soil structure do not come out as the mere summation of strengths and rigidities of soils and geosynthetics. They appear as a result of mechanical interaction between soils and geosynthetics. Ohta et al. (1996, 1998) constructed a series of trial embankments that were reinforced by geosynthetics and tried to examine geosynthetic-reinforcement effect.

This paper aims at numerically examining the geosynthetic-reinforcement mechanism. Herein, the soil which is compacted is modeled by the subloading surface Sekiguchi and Ohta's elasto-plastic constitutive model, in which the subloading surface proposed by Hashiguchi(1989) is introduced. This model is capable of expressing the dilatancy characteristics when the current stress state is located inside the yielding surface. The authors believe that confining the dilative deformation of compacted soils by reinforcements such as geosynthetics would be a key in the reinforcing mechanism.

2 Experiments

2.1 Full scale in-situ model test

A full scale in-situ model test (July, 20-August, 8, 1992 in Kanazawa, Japan) was performed in order to investigate the reinforcing mechanism by geosynthetics (Ohta et al., 1996; 1998). A beam shaped soil structure reinforced by geosynthetics was designed and the resisting capability of structure against the bending moment was also investigated.

The soil used in the experiment was Omma sand. The specific gravity of soil particle was 2.71, and the distribution of grain size corresponds to 89.3% of san fraction(75 μm to 2mm).

The schematic plot of test embankment having the supporting beams is shown in Fig.1(a), which consists of 2.75m in height, 42.5m in length and 4.5m in width, respectively. At the construction of test embankment, soil was spread over up to 10cm thickness and compacted sufficiently by a vibration roller. The degree of compaction was controlled by a dry unit weight which was measured by RI(radioisotope) method. Geosynthetics (Adem#G-6, Maeda Kohsen Co.) was placed per every 50cm. The experiment started by removing the steel H piles, which were supporting the reinforced portion by geosynthetics, and it was organized as shown in Fig.1(b). The deformation of the reinforced soil structure was measured by photographic observation of the position changes of markers installed at every 25 cm interval on the side of embankment. In the experiment, when #10 steel H pile was removed at step 9, the structure was failed.

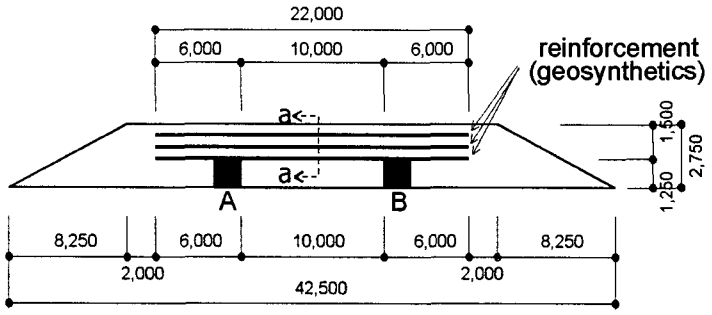

(a) Side view of test embankment

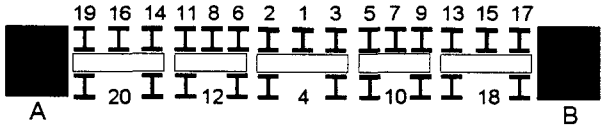

(b) Position of supporting steel H piles

Fig. 1 Embankment schematic drawing(unit: mm)

2.2 Laboratory tests(Constant volume shear box test (CV-SBT))

Mechanical properties of soil such as used in the experiment, compressibility and shear, were investigated as previously said. A series of shear box tests were carried out for both completely disturbed remolded (loose) samples and compacted undisturbed (dense) samples. The specimen was set in a shear box (6.0 cm in diameter and 2.0 cm in height) and sheared under the condition of constant volume after being consolidated by a designated vertical pressure a designated vertical

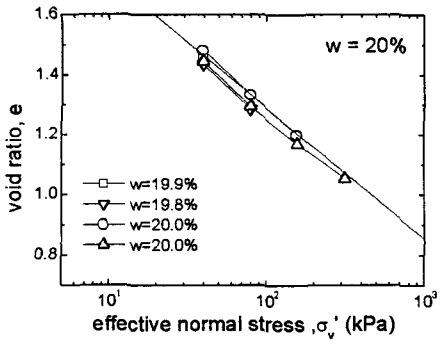

(a) Compression properties

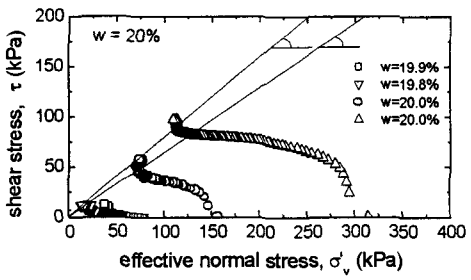

(b) Shear properties

Fig. 2 Mechanical properties of disturbed sample from CV-SBT

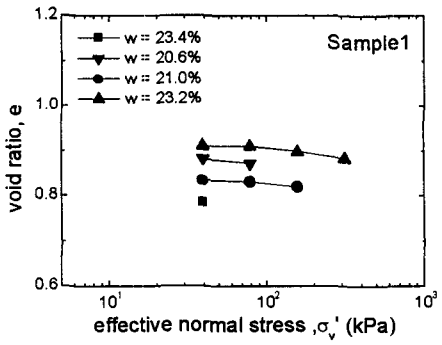

(a) Compression properties

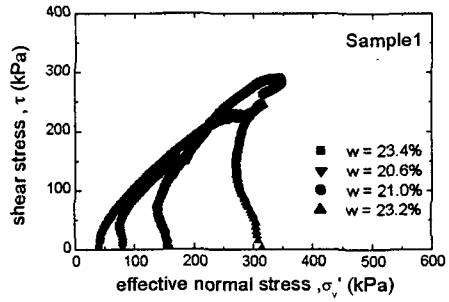

(b) Shear properties

Fig. 3 Mechanical properties of undisturbed sample from CV-SBT

pressure,

Compressibility of remolded (loose) samples is shown in Fig.2(a) and the effective stress paths under shearing are depicted in Fig.2(b). The initial water content of each sample is also denoted in Fig.2(b). Likewise, compressibility and shear characteristics of compacted undisturbed (dense) samples are shown in Figs.3(a) and (b), respectively. In the figure, we note that the disturbed samples behave like normally consolidated clays, on the contrary, the compacted undisturbed samples behave like over-consolidated clays. We think that the constitutive models which can explain the dilation of soil element are applicable to the compacted soils, when the effective stress paths in Fig.3(b).

3. An elasto - plastic modeling of compacted soils

Therefore, we introduce the conventional an elasto-plastic constitutive model(Sekiguchi and Ohta ,1977) and the subloading surface concept(Hashiguchi, 1989) to understand the mechanical behavior inside the normal yielding surface. The constitutive model by Sekiguchi and Ohta (1977) can be regarded as an extension of the original Cam clay model but is distinguished from the Cam-clay model on description ability of the mechanical behavior, which arose from initial anisotropy and stress reorientation. The determination procedure of input parameters needed in the constitutive model has been well established (Iizuka and Ohta, 1987) through a lot of practical case studies

using a finite element code, DACSAR, which is employed in the Sekiguchi and Ohta's model (Iizuka and Ohta, 1987 and Mestat, 2001).

3.1 Sekiguchi and Ohta's model with subloading surface

The normal yielding function of the Sekiguchi and Ohta's model(SO model) is expressed as,

$$f=\frac{\lambda-k}{1+e_0}\ln\frac{p'}{p'_0}+D\,\eta^*-\varepsilon_v^p=0 \tag{1}$$

in which D is the coefficient of dilatancy proposed by Shibata(1968), ε_v^p is the volumetric strain, $\lambda(=0.434C_c)$ and $k(=0.434C_s)$ are compression and swelling indices, respectively. The parameters of λ, k and D have a theoretical relation with the critical state parameter, M, as $M=\frac{\lambda-k}{D(1+e_0)}$ (Ohta, 1971). η^* is the generalized deviatoric stress parameter defined as,

$$\eta^*=\frac{3}{2}\left\|\frac{\mathbf{s}}{p'}-\frac{\mathbf{s}_0}{p'_0}\right\| \tag{2}$$

in which $\mathbf{s}$ is the deviatoric stress tensor, the subscript 0 denotes the value at the reference and $\|\cdot\|$ is the Euclid norm. After Hashiguchi(1989), the subloading surface f_s similar to the normal yielding surface can be defined using the similarity ratio R as,

$$f_s=\frac{\lambda-k}{1+e_0}\ln\frac{p'}{p'_0}+D\,\eta^*-\left(\varepsilon_v^p+\frac{\lambda-k}{1+e_0}\ln R\right)=0 \tag{3}$$

in which the similarity ratio R determines the scale of subloading yielding surface against the normal yielding surface and is defined as $\frac{p'}{\bar{p}'}$ using the current effective mean stress, p' at the subloading yielding surface and its conjugate effective mean stress, $\bar{p}'$ at the normal yielding surface. The evaluation law of the similarity ratio, R is assumed as,

$$\dot{R}=U_R\|\dot{\boldsymbol{\epsilon}}^p\|=-\frac{m}{D}(\ln R)\|\dot{\boldsymbol{\epsilon}}^p\| \qquad \text{for} \quad \dot{\boldsymbol{\epsilon}}^p\neq\mathbf{0} \tag{4}$$

after Hashiguch(1989), in which m is the newly introduced material parameter controlling the accessibility rate of the subloading surface to the normal yielding surface. Herein, note that the scalar function, U_R is defined in the region of $0<R\leq 1$ and satisfies $U_R=\infty$ when $R=0$ and $U_R=0$ when $R=1$. Since the current effective stress always stay on the subloading surface, the consistency condition can be described as $\dot{f}_s=0$.

3.2 Calibration of modeling

In this section, the simulation of shear behavior obtained from SBT under the condition of constant volume is presented. The input parameters are determined from the compression test and the shear test results for disturbed sample (Fig.2 (a) and (b)). The stress ratio, $(\tau/\sigma'_v)_f$ a at the critical state in case of the direct shearing such as the shear box test under the condition of constant volume, can be derived by simultaneously solving the critical state condition, $\beta=0$ and the underained (constant volume) condition, $\dot{\epsilon}_v(=\dot{\epsilon}_v^e-\dot{\epsilon}_v^p)=0$ of Sekiguchi and Ohta's model as (Ohta et al., 1993 and Morikawa., 1997),

$$\left(\frac{\tau}{\sigma'_v}\right)_f=\frac{1+2K_0}{3\sqrt{3}}M \tag{5}$$

With the help of empirical relation of $K_0=1-\sin\phi'$(Jaky, 1944), the critical state parameter, M can be expressed by $(\tau/\sigma'_v)_f$ because of $M=\frac{6\sin\phi'}{3-\sin\phi'}$. The experimental value of $(\tau/\sigma'_v)_f$ is given in Fig.2(b) though little difference is found in the critical state lines with the water content. Two critical state lines can be drawn by solid lines as shown in Fig.2 (b) depending on which point, the final point or the kink point, on the effective stress path should be taken as the critical state. Herein, the kink point of effective stress path is chosen as the critical state point and then the critical state parameter, M is determined to be 1.73. The compression index, $\lambda\ (=0.434C_c)$ can be directly determined to be 0.195 from Fig. 2(a) because it is known that the gradient of compression line from K_0 consolidation in the $e-\ln p'$ relation coincide each other (e.g., Mitachi and Kitago, 1976). And the irreversible ratio Λ is assumed 0.5. Thus, the determination procedure can be summarized as in Fig.4 after Hirata et al. (1999).

However, the parameter, m, there is no way to directly determine it from the test results at the present stage. Then, in this paper, a series of parametric studies are carried out and the trial of estimating the value of the constitutive model reduces the original Sekiguchi and Ohta's model which does not have subloading surface is determined to be 0.001. Herein, in case that which gives the best fit to the effective stress paths obtained from CV-SBT as shown in Fig.5.

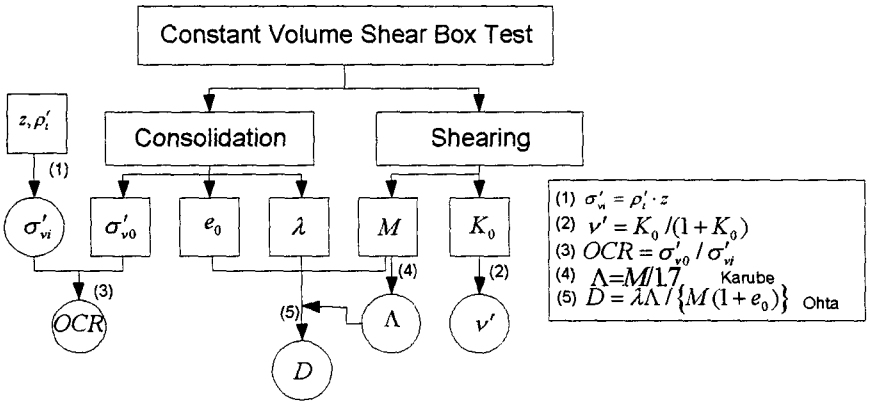

Fig. 4 Specification procedure of parameter

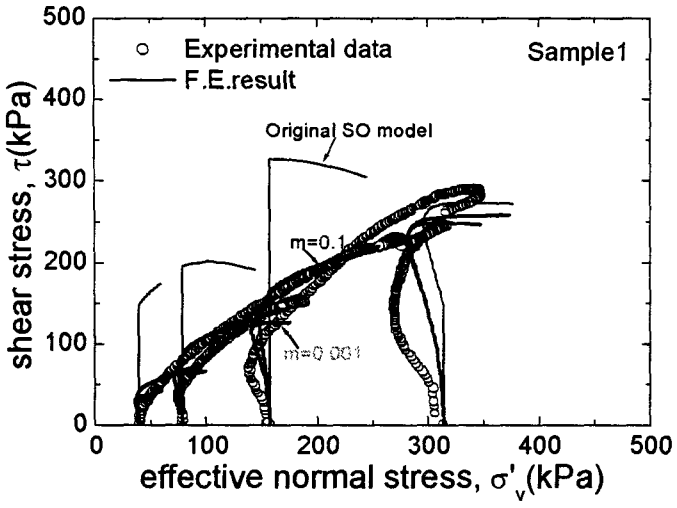

Fig. 5 Computed stress paths of compacted soil

4. Reinforcement (Geosynthetics)

Figure 6 shows the experimental result of uniaxial extension test for geosynthetics materials used in field model test. The linearly elastic model is applied to represent the stress and strain relationship of geosynthetics, and the bar elements in F.E. simulation are also employed. In numerical prediction, the bar elements are treated as no resistance materials against axial compression in the Fig.7. The extension strength is 67.3 kN/m, the cross sectional area is 5.25×10^{-4} m^2 and Young's modulus is 2.55×10^{6} kPa, respectively.

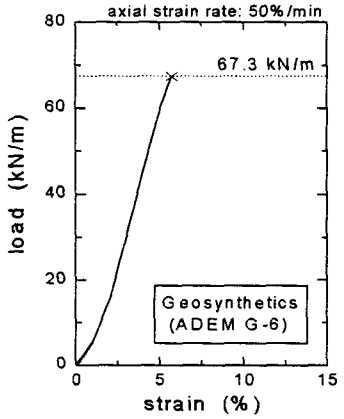

Fig. 6 Stress-strain relation of geosynthetics

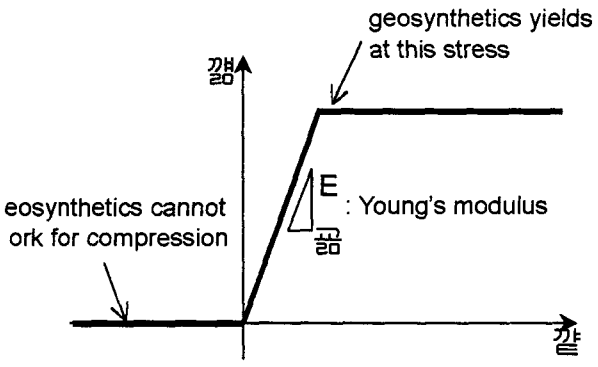

Fig. 7 Geosynthetics model(bar element)

5. Finite Element Simulation

The finite element mesh employed in the simulation of the full-scale in-situ model test is shown in Fig.8. The 4-node constant strain finite element and the forward incremental calculation scheme are used. The dead load of reinforced soil structure is applied as external forces being downward loaded at the bottom nodal points where the supporting H steel is removed in order at experiment. In the simulation, three cases are considered regarding OCR (OCR=1, 10 and 50).

In Figure 9, numerical predictions and monitored behaviors are compared in which the horizontal axis in the figure represents step number shown in Fig.8. Labels G1, G2 and G3 indicate location of geosynthetics placed; G1 is lower layer, G2 is middle layer and G3 is upper layer, respectively. As seen from the figures, monitored deformations are somewhat larger than numerical predictions. We think it would be because geosynthetics hung down at experiment when the support was removed and then soils between geosynthetics were loosened.

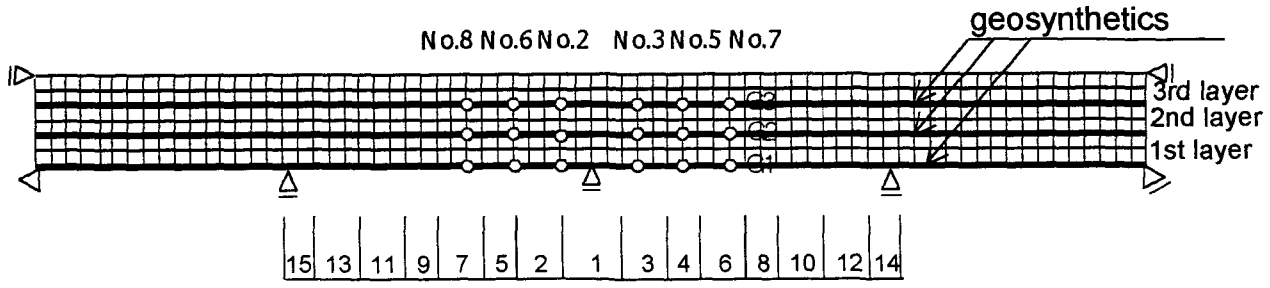

Fig. 8 Finite element mesh employed in numerical prediction

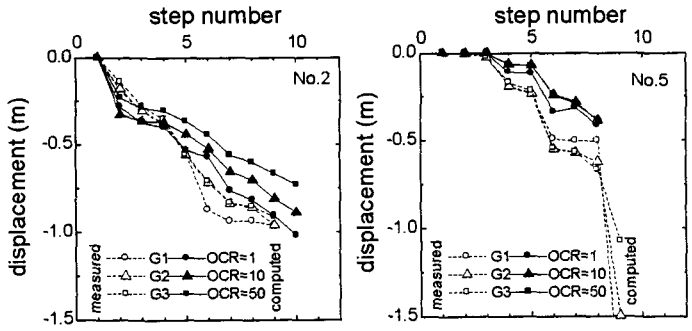

Fig. 9 Computed and monitored deformations

6. Conclusions

The monitored behavior of the full-scale model test and its numerical predictions are compared. Particularly the mechanical interaction between the compacted soils and the geosynthetic-reinforcement materials is emphasized as a benchmark that should be taken into consideration in analyzing the geosynthetic-reinforcement effect. Major items presented in this paper are summarized as follows.

① The elasto-plastic constitutive modeling with the subloading surface is introduced to describe the mechanical behavior of compacted soils and its applicability to the compacted soils is examined.
② The dilatancy characteristics of compacted soils depending on the degree of compaction are discussed.
③ A practical procedure determining input parameters needed in the analysis of geosynthetic-reinforcement effect is proposed.
④ A series of elasto-plastic finite element simulation is performed and the applicability of the simulation technique to the analysis of the geosynthetic-reinforcement mechanism is examined by comparing the computed prediction with the measured results.

References

1. Kenney,T.C. (1959), Discussion on Proc. Paper 1732(Wu, 1958), Proc.ASCE,Vol.85,SM3,pp.67-69.
2. Hashiguchi,K. and Ueno,M.(1977), "Elasto-plastic constitutive laws of granular materials, Constitutive Equations of Soils" , Proc. Spec. Session 9 of 9th ICSMFE, Murayama, S. and Schofield, A.N.(eds.), Tokyo, JSSMFE, pp. 72-82.
3. Hashiguchi,K.(1989), "Subloading surface model in unconventional plasticity, International jour. Of Soils and Structures" , Vol. 25, pp.917-945.
4. Hirata, M., Izizuka,A.,Ohta,H.,Yamakami,T., Yokota,Y. and Ohmori, K. (1999), "The numerica simulation of geosyntheics-reinforced soil structure using elasto-plastic dilatancy m Journal of JSCE, No.631/V-48,pp.179-192(in Japanese)
5. Iizuka,A. and Ohta,H.(1987), "A determination procedure of input parameters in elasto-viscoplastic finite element analysis" , Soils and Foundations, Vol.27, No.3, pp.71-87.
6. Jaky, J.(1944), Tarajmechanika, J. Hungarian Arch. And Engs., Budapest, pp.355-358.
7. Massarsch,K.R.(1979), "Lateral Earth pressure in normally consolidated clay" , Design Parameters in Geotechnical Engineering, Proc. 7th European. Conference of Soil Mechanics and Foundation Engineering, Vol.2, pp.245-249.
8. Ohta,H. Goren,S., Iizuka,A. Yamakami,T. Yamagishi,K., and Moroto,N.(1996), "Numerical simulation of beam-shaped soil structure reinforced by Geosynthetics" , Proc. Of Int. Symposium on Earth Reinforcement, Balkema, Vol.1, pp.255-260.
9. Ohta,H. Hirata,M. Iizuka,A. Yamakami,T. Yokota,Y. Ohmori,K.(1998), "Application of Dilatancy Models to Soils Reinforced by Geosynthetics" , Sixth International Confernce on Geosynthetics , 551-556.
10. Sekiguchi,H. and Ohta,H.(1977), "Induced anisotropy and time dependency in clays" , Proc. Specialty Session 9, 9th Int. Conf. Soil Mechanics and Foundation Engineering, Tokyo, pp.229-239.